Soft Matter

Accepted Manuscript

ROYAL SOCIETY OF CHEMISTRY

www.rsc.org/softmatter

ARTICLE TYPE www. rsc.org/xxxxxx | XXXXXXXX

Influence of wetting on fingering patterns in lifting Hele-Shaw flows

Pedro H. A. Anjos[a] **and José A. Miranda,**[b]

Received Xth XXXXXXXXXX 20XX, Accepted Xth XXXXXXXXX 20XX
First published on the web Xth XXXXXXXXXX 200X
DOI: 10.1039/b000000x

We study the pattern formation dynamics related to the displacement of a viscous wetting fluid by a less viscous nonwetting fluid in a lifting Hele-Shaw cell. A perturbative weakly nonlinear analysis of the problem is presented. We focus on examining how wetting effects influence the morphology of the emerging interfacial patterns at the early nonlinear regime. Our analytical results indicate that wettability has a significant impact on the resulting nonlinear patterns. It restrains finger length variability while inducing the development of structures presenting short, blunt penetrating fingers of the nonwetting fluid, alternated by short, sharp fingers of the wetting fluid. The basic mode-coupling mechanisms leading to such behaviors are discussed.

1 Introduction

It is known that wetting effects are of relevance in the development of pattern formation structures that arise as a result of hydrodynamic instabilities [1–4]. In particular, this is true for the Saffman-Taylor instability [5], that occurs when a less viscous fluid displaces a more viscous one in the confined geometry of a Hele-Shaw cell [6–8]. The fact is that, depending on the nature of the fluids involved they can wet the walls of the Hele-Shaw cell plates, leaving behind a film of finite thickness. In a seminal paper [9] Park and Homsy have shown that the consideration of such wetting effects leads to nonnegligible corrections in the pressure difference at the fluid-fluid interface. A number of subsequent theoretical and experimental investigations in rectangular Hele-Shaw cells [10–14] have indicated that the inclusion of wetting effects helps to provide a better match between theory and experiments. This has also been the case for injection-driven flows in the radial Hele-Shaw cell setup [15–17]. Recently, it has also been proposed that the traditional "fanlike" patterns obtained in radial flows [18–22] which present fingers that bifurcate and compete, would be substituted by stubby fingers of similar lengths, when wetting effects are of significance [23].

Actually, there is another Hele-Shaw cell-type problem in which the influence of wetting is quite important. It is referred to as the rotating Hele-Shaw setup [24]. In this situation, the interface instability is not driven by the viscosity contrast between the fluids, but rather by the difference in their densities. In this version of the problem the inner fluid has a larger density, and the Hele-Shaw cell is allowed to rotate about an axis perpendicular to the plates. Within this context, an interplay between surface tension and centrifugal forces leads to the formation of a variety of pattern morphologies [25–29] that are very different from the ones detected in viscosity-driven flows. A particularly nice study has been performed in Ref. [30], which considered the relevance of wetting in fingering patterns produced in a rotating Hele-Shaw cell. Their fully nonlinear numerical simulations and experiments have demonstrated that wetting effects have a strong impact on the resulting interfacial morphologies. An interface stabilization due to dynamic wetting has also been disclosed.

A third system involving a variant of the usual injection-driven Saffman-Taylor instability that has been extensively studied over the past fifteen years or so is the lifting Hele-Shaw cell problem [31]. In contrast to the injection-driven and centrifugally-induced circumstances discussed above, in this modified arrangement the upper cell plate can be lifted, in such a way the cell gap-width is time-dependent. As the plates separate, the pressure becomes lower in the inner more viscous fluid, and the outer fluid moves in. Then, the fluid-fluid interface rapidly deforms, and peculiar treelike patterns arise [32–38]. Here the most prominent pattern-forming mechanism is finger competition among the fingers of the invading less viscous fluid. Moreover, these invading fingers are typically wider than the outward pointing fingers of the more viscous fluid.

In spite of the relatively large number of investigations of the lifting Hele-Shaw problem (see [31–38] and references therein), the influence of wetting films on the dynamics of finger competition, and also on the shape of both inward and outward pointing fingers has been overlooked. Just a few groups investigated the role of fluid wettability on the lifting Hele-Shaw problem [36,39,40]: the early linear dynamic stage problem has been theoretically investigated in Refs. [36,39], while Ref. [40] concentrated on analyzing experimentally the interplay of wetting and other substrate properties at advance time

[a] *Departamento de Física, Universidade Federal de Pernambuco, Recife, Pernambuco 50670-901 Brazil. E-mail: pedroanjos@df.ufpe.br*
[b] *Departamento de Física, Universidade Federal de Pernambuco, Recife, Pernambuco 50670-901 Brazil. Fax: 55 81 2126 8450; Tel: 55 81 2126 7610; E-mail: jme@df.ufpe.br*

stages of pattern formation. The linear stability analyses performed in [36,39] focused on showing that wetting effects are important to allow better theoretical predictions about the number of fingers at the onset of the instability. Therefore, the role played by wetting film effects on intrinsically nonlinear phenomena related to finger competition events, and on the morphology of individual fingers could not be assessed. Motivated by this fact, in this work we carry out a perturbative weakly nonlinear analysis of the lifting Hele-Shaw problem which offers useful analytical insights into the influence of the wetting film on the emerging fingering structures.

Before we proceed, it should be noted that while in Ref. [23] we have investigated the influence of wetting thin films on the patterns generated for injection-driven flows in constant-gap Hele-Shaw cells, here we focus on examining the role of wettability on the patterned structures which arise during lifting flows in a variable-gap Hele-Shaw setup. It is well known that the resulting nonlinear pattern morphologies in the usual injection-driven Hele-Shaw case are very different from the ones obtained in the lifting Hele-Shaw problem. For instance, phenomena like finger tip-splitting are very frequent in the injection-driven problem, but are completely absent in the lifting case [32–38]. Moreover, in contrast to the injection-driven case (where pressure is Laplacian) the pressure field in the lifting flow situation is non-Laplacian [31]. In addition, the own nonlinear nature of both problems does not allow one the make *a priori* predictions about possible similarities in the response of both systems to wetting film effects. Finally, to the best of our knowledge, a study about the role of wetting in lifting Hele-Shaw systems is still lacking. All these facts motivated us to perform our current study.

The rest of this paper is organized as follows. In Sec. 2 we use a perturbative weakly nonlinear approach originally proposed in Refs. [20,41] to obtain a mode-coupling differential equation that describes the time evolution of the interfacial perturbation amplitudes up to second-order. We concentrate our attention on the incorporation of wetting film effects into the lifting Hele-Shaw problem, and examine how wettability influences the intrinsically nonlinear mechanisms of the pattern-forming dynamics. Contrary to purely linear stability analyses, which mainly provide information about the stability on the fluid-fluid interface, our weakly nonlinear approach permits analytical assess to the morphology of the patterns at the early nonlinear regime. The role played by the wetting thin film in regulating these important nonlinear aspects is discussed in Sec. 3. Finally, Sec. 4 presents our concluding remarks.

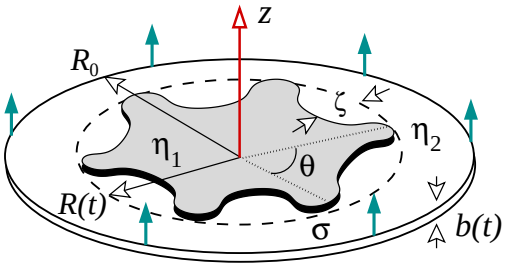

Fig. 1 Representative sketch of the lifting flow in a radial Hele-Shaw cell.

2 Governing equations and weakly nonlinear calculation

We consider a Hele-Shaw cell of a time-dependent gap width $b(t)$ containing a more viscous fluid of viscosity η_1, surrounded by a less viscous fluid of viscosity η_2 [Fig. 1]. The fluids are Newtonian and immiscible, and the surface tension between them is denoted by σ. The upper cell plate can be lifted along the direction perpendicular to the plates (z-axis), and the lower plate is held fixed. The initial fluid-fluid interface is circular, having radius $R_0 = R(t=0)$ and initial gap thickness $b_0 = b(t=0)$. By using volume conservation the time dependent radius of the unperturbed interface is given by

$$R(t) = R_0 \sqrt{\frac{b_0}{b(t)}}. \tag{1}$$

As in Refs. [9–17] our weakly nonlinear theory is developed with the assumption that fluid 1 wets the walls of the Hele-Shaw cell, leaving behind a thin wetting film. Fluid 2 is nonwetting.

Since during the lifting process a less viscous fluid pushes a more viscous one, the Saffman-Taylor instability takes place, and the fluid-fluid interface deforms. The perturbed fluid-fluid interface is described as $\mathscr{R}(\theta,t) = R(t) + \zeta(\theta,t)$, where θ represents the azimuthal angle. Here, $\zeta(\theta,t) = \sum_{n=-\infty}^{+\infty} \zeta_n(t) \exp(in\theta)$ is the net interface perturbation with Fourier amplitudes $\zeta_n(t)$, and discrete wave numbers n. Our perturbative approach keeps terms up to the second-order in ζ. In the Fourier expansion of ζ we include the $n=0$ mode to maintain the area of the perturbed shape independent of the perturbation ζ. Mass conservation imposes that the zeroth mode is written in terms of the other modes as $\zeta_0 = -(1/2R) \sum_{n\neq 0} |\zeta_n(t)|^2$.

In the lifting Hele-Shaw cell setup the flow is governed by two equations: a gap-averaged Darcy-law [5–8]

$$\mathbf{v}_j = -\frac{b^2(t)}{12\eta_j} \nabla p_j, \tag{2}$$

and the gap-averaged incompressibility condition[31]

$$\nabla \cdot \mathbf{v}_j = -\frac{\dot{b}(t)}{b(t)}. \quad (3)$$

In Eq. (2) $\mathbf{v}_j = \mathbf{v}_j(r,\theta)$ and $p_j = p_j(r,\theta)$ denote the velocity and pressure in fluids $j = 1,2$, respectively. Moreover, in Eq. (3) $\dot{b}(t) = db(t)/dt$ is the upper plate velocity along the z-axis. As in most experimental and theoretical studies in lifting Hele-Shaw flows[32–38] we consider a constant lifting speed $\dot{b}(t) = \dot{b} = V$, so that $b(t) = b = b_0 + Vt$.

At this point we briefly comment on the validity of the gap-averaged Darcy's law description for the lifting Hele-Shaw problem. Despite the intrinsic three-dimensional nature of the problem, one should consider that the upper plate is not being lifted fast enough to provoke any inertial effects, nor lifted high enough to alter the system being of large aspect ratio[31,39]. The gap width $b(t)$ is always far smaller than the radius of the unperturbed fluid-fluid interface $R(t)$, so that $R(t)/b(t) \gg 1$. As a matter of fact, this is precisely the flow regime investigated by laboratory experiments in lifting Hele-Shaw cells[32–38]. The reliability of the gap-averaged effectively-two-dimensional approach is further substantiated by the similarity between the numerical simulations employing Darcy's law equations with the corresponding interfacial patterns obtained experimentally[31,37,38]. In these studies it has been found that the Darcy's law model satisfactorily accounts for the initial, intermediate, and fully nonlinear evolution of the observed fingering patterns.

From the irrotational nature of the flow ($\nabla \times \mathbf{v}_j = 0$) one can define a velocity potential ϕ_j ($\mathbf{v}_j = -\nabla\phi_j$). It can be readily verified that ϕ_j obeys the Poisson equation $\nabla^2\phi_j = \dot{b}/b$, having the solution

$$\phi_j(r,\theta) = \frac{\dot{b}r^2}{4b} + \sum_{n\neq 0} \phi_{jn}(t) \left(\frac{r}{R}\right)^{(-1)^{(j+1)}|n|} e^{in\theta}. \quad (4)$$

To find a relation between $\phi_{jn}(t)$ and $\zeta_n(t)$, we apply the kinematic boundary condition

$$\frac{\partial \mathscr{R}}{\partial t} = \left(\frac{1}{r^2}\frac{\partial \mathscr{R}}{\partial \theta}\frac{\partial \phi_j}{\partial \theta}\right) - \left(\frac{\partial \phi_j}{\partial r}\right), \quad (5)$$

which states that the normal components of each fluid's velocity are continuous at the interface[6–8,18].

The contributions coming from surface tension and wetting effects are included in a generalized Young-Laplace pressure boundary condition, which expresses the pressure jump across the fluid-fluid interface[9–17,23,30]

$$p_1 - p_2 = \frac{\pi}{4}\sigma\kappa + \frac{2\sigma}{b}\left[\cos\theta_c - J\left(\frac{\eta_1 v_n}{\sigma}\right)^{\gamma}\right]. \quad (6)$$

The first term on the right-hand side (RHS) of Eq. (6) represents the contribution related to surface tension and the interfacial curvature κ in the plane of the Hele-Shaw cell. The factor $\pi/4$ is purely a capillary static effect, coming from the z-average of the mean interfacial curvature. The second term on the RHS of Eq. (6) accounts for the contribution of the constant curvature associated with the interface profile in the direction perpendicular to the Hele-Shaw cell plates, set by the static contact angle θ_c measured between the plates and the curved meniscus. Recall that we consider a nonwetting fluid (fluid 2) displacing a wetting one (fluid 1), so that $\theta_c = \pi$. Finally, the third term on the RHS of (6) considers the effect of a thin wetting film trailing behind the displaced fluid, where v_n is the normal component of the interface velocity, $J = 3.8$, and $\gamma = 2/3$. This third term is crucial to this paper, and it has been originally proposed by a prior theoretical work by Park and Homsy[9]. They were the first to conduct such a theoretical analysis by combining Bretherton's lubrication approximation[42] with the Saffman-Taylor equations[6], via double asymptotic expansion of the ratio of film thickness to transverse characteristic length and capillary number raised to 1/3. Following Park and Homsy's analysis existing experimental and theoretical results were reconciled, thereby elucidating the important role of wetting film in the nonlinear finger formation process.

It should be noticed that in the lifting Hele-Shaw flow all parts of the fluid-fluid front recede. This fact is clearly illustrated in Fig. 4 of Ref.[38], and in Figs. 2, 3, and 8 in Ref.[37]. This situation is very different to what happens in rotating Hele-Shaw flows[30], where some parts of the front recede while others advance. In this last case the advancing portions explore dry regions of the plates, and the contact angle should be treated as a dynamic variable.

Following canonical steps performed in previous weakly nonlinear studies for Hele-Shaw flows[20,41], first we define Fourier expansions for the velocity potentials. Then, we express ϕ_j in terms of the perturbation amplitudes ζ_n by considering condition (5). Substituting these relations, and the pressure jump condition Eq. (6) into Darcy's law Eq. (2), always keeping terms up to second-order in ζ, and Fourier transforming, we find (after some algebra) the equation of motion for the perturbation amplitudes (for $n \neq 0$)

$$\begin{aligned}\dot{\zeta}_n &= \lambda(n)\zeta_n \\ &+ \sum_{n'\neq 0}\left\{F(n,n')\zeta_{n'}\zeta_{n-n'} + G(n,n')\dot{\zeta}_{n'}\zeta_{n-n'}\right. \\ &+ \left. H(n)\left[\dot{\zeta}_{n'}\dot{\zeta}_{n-n'} + \frac{\dot{b}}{2b}\zeta_{n'}\dot{\zeta}_{n-n'}\right]\right\}, \end{aligned} \quad (7)$$

where

$$\lambda(n) = \frac{1}{1+w(n)}\left[-\frac{\dot{b}}{2b}(1+A|n|) - \frac{\pi\sigma b^2(1-A)}{96\eta_1 R^3}|n|(n^2-1)\right], \quad (8)$$

is the linear growth rate, $A=(\eta_2-\eta_1)/(\eta_2+\eta_1)$ is the viscosity contrast, and

$$w(n) = \gamma|n|J\frac{(1-A)}{12}\frac{b}{R}\left(\frac{2b\sigma}{\dot{b}\eta_1 R}\right)^{1-\gamma} \quad (9)$$

is related to the wetting film contribution.

The second-order mode-coupling terms are given by

$$F(n,n') = \frac{1}{1+w(n)}\left\{\frac{|n|}{R}\left[\frac{A\dot{b}}{2b}\left[\frac{1}{2}-\mathrm{sgn}(nn')\right] - \frac{\pi b^2\sigma(1-A)}{96\eta_1 R^3}\left[1-\frac{n'}{2}(3n'+n)\right]-\frac{\dot{b}}{2b}\frac{1}{|n|}\right] + \frac{\dot{b}}{2b}\frac{w(n)}{2R}n'(n-n')\right\}, \quad (10)$$

$$G(n,n') = \frac{1}{1+w(n)}\left\{\frac{1}{R}\left[A|n|[1-\mathrm{sgn}(nn')]-1\right] - \frac{w(n)(\gamma-1)}{2R}\right\}, \quad (11)$$

and

$$H(n) = \frac{w(n)}{1+w(n)}\frac{b}{\dot{b}R}(\gamma-1), \quad (12)$$

where the sgn function equals ± 1 according to the sign of its argument.

The expressions (7)-(12) represent the mode-coupling equations of the viscous fingering problem in a lifting Hele-Shaw cell, taking into consideration the contributions from wetting film effects. As commented in Sec. 1, this set of coupled nonlinear equations opens up the possibility of investigating analytically how the morphology of the evolving fluid-fluid interface responds to the action of thin film wettability. It should be noted that the linear growth rate [Eqs. (8) and (9)] was originally obtained in Ref.[39]. Note that the situation in which wetting effects are neglected can be readily obtained by setting $\gamma=0$. In this case we do recover the linear growth rate derived in the literature in the absence of wetting effects[31,36].

3 Wetting film effects - Weakly nonlinear behavior

This section demonstrates the usefulness of our weakly nonlinear analysis in elucidating key aspects related to finger shape behavior and finger competition under the action of wetting film effects. We use our mode-coupling approach to investigate the interface evolution at second-order. At this point, it is convenient to rewrite the net perturbation ζ in terms of cosine and sine modes

$$\zeta(\theta,t) = \zeta_0 + \sum_{n=1}^{\infty}\left[a_n(t)\cos(n\theta)+b_n(t)\sin(n\theta)\right], \quad (13)$$

where $a_n=\zeta_n+\zeta_{-n}$ and $b_n=i(\zeta_n-\zeta_{-n})$ are real-valued. Without loss of generality we may choose the phase of the fundamental mode so that $a_n>0$ and $b_n=0$.

In order to maintain our theoretical analysis as close as possible to real life lifting Hele-Shaw experimental studies, we emphasize that the values we take for our parameters throughout the rest of this work are consistent with typical physical quantities used in such experiments[31–38]. For an exhaustive listing of all typical values of the relevant physical quantities we refer the reader to table I presented in Ref.[38]. There one can verify that the lifting Hele-Shaw experiments use highly viscous fluids [with viscosities as high as 101.7 Pa s], and very small initial gap spacings [as small as 1μm]. Here we consider the growth of fingers in the most unstable situation ($A\to -1$), as air [$\eta_2\approx 0$] displaces a very viscous silicone oil [$\eta_1\approx 100$ Pa s]. The initial thickness of the cell b_0= 50 μm and the surface tension between the fluids σ= 0.02 N/m. Moreover, the lifting velocity V=2.5 μm. The initial radius $R_0=3.0\times 10^{-3}$ m and the evolution of the interfaces we consider run up to time $t=19$ s.

In a popular review article, Homsy[6–8] has identified the main growth mechanisms of the viscous fingering process in injection-driven Hele-Shaw flows as being spreading, splitting, and competition. Some time ago Miranda and Widom[20,41] have shown that these basic mechanisms could be consistently mimicked by considering the weakly nonlinear coupling of just a few participating modes: finger competition events (or, finger length variability) could be described by the interaction of a fundamental mode n and its sub-harmonic $n/2$, while the shape of the fingers (finger widening and narrowing) could be given by the interplay between the fundamental mode n, and its first-harmonic $2n$. Here we use this simple picture in order to get some insight into the morphology and early nonlinear features of the patterns generated in a lifting Hele-Shaw cell, when wetting effects are neglected ($\gamma=0$, see Fig. 2), and when wetting effects are of relevance ($\gamma=2/3$, see Fig. 3).

Figures 2 and 3 are plotted by considering the simultaneous coupling of the Fourier modes $n=20$, $n/2=10$, and $2n=40$. We take the initial amplitudes as $a_n(0)=R_0/1000$, $a_{n/2}(0)=$

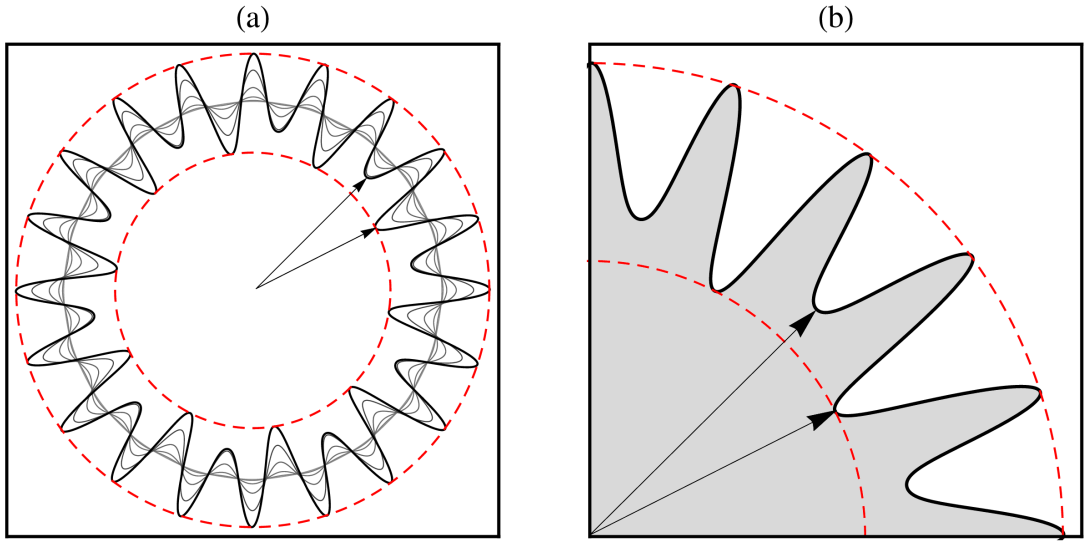

Fig. 2 (a) Snapshots of the evolving interface, plotted at equal time intervals for the interaction of the fundamental mode n, its sub-harmonic $n/2$, and its first-harmonic $2n$, when wetting effects are not present ($\gamma = 0$). Darker colors mean later times. The dashed curves are added to better guide the eye regarding finger competition events. The arrows indicate the radial position of inward pointing fingers. (b) Close-up view (angular sector $0 \leq \theta \leq \pi/2$) of the resulting interface.

$b_{n/2}(0) = R_0/3000$, and $a_{2n}(0) = 0$. In (a), the interfaces are plotted for $0 \leq t \leq 19$ s, at equal time intervals $\Delta t = 3.8$ s. In (b) close-up sections of the interfaces (angular sector $0 \leq \theta \leq \pi/2$) at the final time $t = 19$ s are shown. This is done to facilitate visualization and offer more details about the final interfacial shapes. The only difference between these figures is that Fig. 2 neglects wetting effects (by setting $\gamma = 0$), while Fig. 3 takes these effects under consideration by taking $\gamma = 2/3$.

It is worth pointing out that the values for the initial perturbation amplitudes used to plot Figs. 2 and 3 are selected in such a way that the amplitudes for the sub-harmonics $a_{n/2}$ and $b_{n/2}$ (responsible for inducing finger competition), and first harmonic a_{2n} (responsible for setting the finger shape as wide or narrow) are considerably smaller than the amplitude of the fundamental mode a_n, so that $a_n(0) > a_{n/2}(0) = b_{n/2}(0)$, and $a_n(0) > a_{2n}(0) = 0$. The initial amplitudes for the sub-harmonic sine and cosine modes are set to be equal to avoid any preferential growth of these modes, while the first harmonic cosine mode is initially set to zero, to let the dynamics dictate its growth and phase as time progresses (as we will see in Sec. 3.2 the first harmonic sine mode does not present nonlinear couplings). Note that the fundamental mode mostly sets the initial n-fold symmetry for the pattern. This is done to avoid artificial growth of modes $a_{n/2}$, $b_{n/2}$, and a_{2n} imposed solely by the initial conditions. This way, the phenomenon of finger competition and finger-broadening we study are spontaneously induced by the weakly nonlinear dynamics, and not by artificially imposing large initial amplitudes for $a_{n/2}$, $b_{n/2}$ and a_{2n}. Moreover, we stress that other combinations for the initial amplitudes (that obey the requirements mentioned above) do result in similar nonlinear features.

Unfortunately, we are not able to perform direct quantitative comparisons between our predicted theoretical weakly nonlinear shapes (as the ones depicted in Figs. 2 and 3) with equivalent interfacial patterns exhibited by real experiments and simulations. The reason for this impediment is that existing laboratory experiments and numerical simulations mostly focus on the fully nonlinear stages of pattern evolution, were the finger sizes are very large, and the finger shapes are considerably complex. For a typical illustration of this fact, see Fig. 3 of a recent lifting Hele-Shaw experiment[38] where at $t' = 25$ an already nonlinear shape is depicted, while at $t' = 10$ ones has a quite unperturbed, initial time, linear morphology (where linear stability analysis applies). In this context, a legitimate weakly morphology could be found for the time interval $10 < t' < 25$, but it is not shown. These remarks are also applied for numerical simulations of the problem (see, for instance, Fig. 3 of Ref.[37]). Our perturbative weakly nonlinear analysis holds at the onset of nonlinearities, where the interfacial disturbances ζ must be significantly smaller than the corresponding unperturbed interfacial radius $R(t)$. Despite its limitations, the weakly nonlinear approach[20] is still useful, in the sense that it can predict analytically the most im-

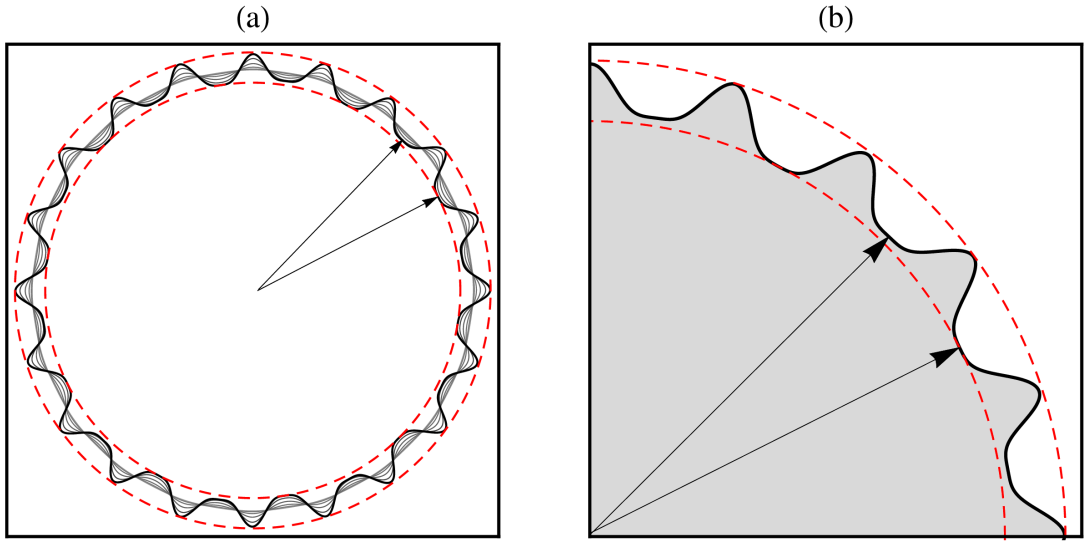

Fig. 3 (a) Snapshots of the evolving interface, plotted at equal time intervals for the interaction of the fundamental , n, its sub-harmonic $n/2$, and its first-harmonic $2n$, when wetting effects are of relevance ($\gamma = 2/3$). Darker colors mean later times. The dashed curves are added to better guide the eye regarding finger competition events. The arrows indicate the radial position of inward pointing fingers. (b) Close-up view (angular sector $0 \leq \theta \leq \pi/2$) of the resulting interface.

portant nonlinear behaviors that will eventually be revealed at advanced time stages of the Hele-Shaw dynamics [27,29].

Having all this in mind, we begin our discussion by examining Fig. 2(a) which considers that $\gamma = 0$: one can see that the inward pointing fingers of the outer fluid present different lengths, indicating the presence of finger competition among them. The dashed circular curves are added to allow a better visualization of the finger competition events: note that some inward pointing fingers of the penetrating fluid touch the inner dashed line, while other inward pointing fingers do not. On the other hand, the fingers of the inner fluid pointing outward have nearly similar sizes (all touch the outer dashed circular curve), indicating that competition among these fingers is repressed. So, the fact is that when wetting effects are neglected, one observes a finger competition phenomenon (presence of fingers of different lengths) among inward pointing fingers (this is clearly indicated by the arrows shown in Fig. 2(a)).

The resulting patterned shape illustrated in Fig. 2(a) shows a quite unstable starburstlike structure where inward moving fingers clearly compete. Moreover, by inspecting the close-up Fig. 2(b) one can actually verify that the inward pointing fingers of the less viscous fluid are just a bit wider than the outward pointing fingers of the more viscous fluid. These two main nonlinear features revealed by Fig. 2 (strong competition among inward pointing fingers, and the fact that they are slightly wider) are in qualitative agreement with the ones detected at more advanced time regimes by experiments and simulations in lifting Hele-Shaw cells [31–38]. However, even though these laboratory and numerical experiments show a clear finger length variability, the observed inward pointing fingers are notably wider than the outward pointing ones.

Now we turn to Fig. 3 which plots (a) the time evolution, and (b) the close-up view of part of the final pattern obtained in the case where the wetting effects are of importance ($\gamma = 2/3$). Recall that all physical quantities (except γ) and initial conditions used to get Fig. 3 are identical to the ones utilized to produce Fig. 2. Inspection of Fig. 3(a) shows that the time evolution under the presence of wetting is considerably different from the equivalent situation that neglected wetting (Fig. 2(a)). One first noteworthy feature is indicated by the arrows, revealing that the finger length variability among inward pointing fingers is reduced as compared to the situation that neglects wetting. This is also true for the outward pointing fingers (all of them touch the external dashed circular curve). We see that even though finger competition of inward pointing fingers is still present in Fig. 3, it is restrained relative to the situation shown in Fig. 2 through the action of wetting effects. It is true that both morphological features (competition and wideness of inward pointing fingers) as shown by Figs. 2 and 3 are still quite small. This is not really surprising since our perturbative mode-coupling theory is only able to access the onset of nonlinear effects.

In addition, the final patterned shape depicted in Fig. 3(b) is clearly different from the starburstlike structure obtained

in Fig. 2(b). Now we observe a more stable pattern formed by shorter fingers, in which wide inward pointing fingers of the penetrating fluid, are alternated by sharp, outward pointing fingers of the inner fluid. Furthermore, the fact that the inward pointing fingers are evidently wider is in better qualitative agreement with the findings of Refs.[31–38] than the case without wetting. When wetting effects are taken into account we end up with patterned structures which present some (but small) competition among inward pointing fingers, that are actually wider than the outward pointing ones. From the analysis of Figs. 2 and 3 we can say that the pattern formation dynamics is evidently sensitive to the wetting condition in the lifting Hele-Shaw problem, and leads to different pattern morphologies.

Although one should not expect to get a quantitative match between the pattern shown in Fig. 3 (that just contains 3 Fourier modes, and is just weakly nonlinear) and the actual fully nonlinear patterns obtained in[31–38], it is reassuring to see that our simple mode-coupling method is able to capture the most salient features of the fully nonlinear dynamics, namely, some competition and clear wideness of inward pointing fingers. In the next two sub-sections we will discuss in a more quantitative way the basic mode-coupling mechanisms leading to the nonlinear morphological behaviors illustrated in Figs. 2 and 3.

3.1 Finger competition behavior

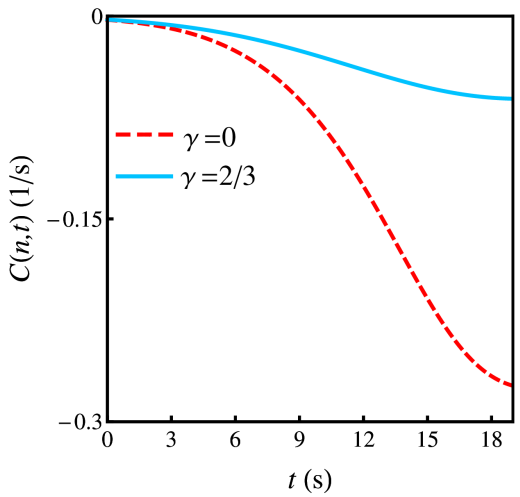

Fig. 4 Time evolution of the finger competition function $C(n,t)$ when wetting effects are neglected ($\gamma = 0$, dashed curve), and when they are taken into consideration ($\gamma = 2/3$, solid curve).

First, we focus on the effects of the wetting film on finger competition events. We follow Ref.[20] and consider finger length variability as a measure of the competition among fingers. Within our approach the finger competition mechanism can be described by the influence of a fundamental mode n, assuming n is even, on the growth of its sub-harmonic mode $n/2$. By using Eqs. (7)-(12) the equations of motion for the sub-harmonic mode can be written as

$$\dot{a}_{n/2} = \{\lambda(n/2) + C(n,t)\}\ a_{n/2}, \tag{14}$$

$$\dot{b}_{n/2} = \{\lambda(n/2) - C(n,t)\}\ b_{n/2}, \tag{15}$$

where

$$\begin{aligned} C(n,t) &= \left\{ \frac{1}{2}\left[F\left(-\frac{n}{2},\frac{n}{2}\right) + \lambda(n/2)\, G\left(\frac{n}{2},-\frac{n}{2}\right)\right] \right. \\ &+ \frac{1}{2}\left[F\left(\frac{n}{2},n\right) + \lambda(n)\, G\left(\frac{n}{2},n\right)\right] \\ &+ \frac{1}{2}\lambda(n)H(n/2)\left[\lambda(n/2) + \frac{\dot{b}}{2b}\right] \\ &+ \left. \frac{1}{2}\lambda(n/2)H(n/2)\left[\lambda(n) + \frac{\dot{b}}{2b}\right]\right\} a_n. \end{aligned} \tag{16}$$

Observing Eqs. (14) and (15), and recalling that $a_n > 0$, we verify that $C(n,t) > 0$ increases the growth of the cosine sub-harmonic $a_{n/2}$, while inhibiting growth of its sine sub-harmonic $b_{n/2}$. The result is an increased variability among the lengths of fingers of fluid 1 pushing the less viscous fluid 2. This effect describes enhanced competition of the outward pointing fingers of fluid 1. Sine modes $b_{n/2}$ would vary the lengths of fingers of fluid 2 penetrating into fluid 1, but it is clear from Eq. (15) that their growth is suppressed if $C(n,t) > 0$.

Reversing the sign of $C(n,t)$ would exactly reverse these conclusions, such that modes $b_{n/2}$ would be favored over modes $a_{n/2}$. Therefore, $C(n,t) < 0$ would indicate increased competition among the inward moving fingers of fluid 2. Regardless of its sign, the magnitude of the function $C(n,t)$ as given by Eq. (16) measures the strength of the competition: increasingly larger values of $C(n,t)$ lead to enhanced finger competition. The validity and correctness of this simple finger competition mechanism during advanced time stages in Hele-Shaw flows has been extensively tested by numerical simulations[27,29].

To examine the influence of wetting effects on the finger competition behavior at second-order, in Fig. 4 we plot $C(n,t)$ as a function of time, considering the absence ($\gamma = 0$) and presence ($\gamma = 2/3$) of a thin wetting film. The parameters used to plot this figure are exactly the ones utilized in Figs. 2 and 3. We consider the coupling between two Fourier modes ($n = 20$ and $n/2 = 10$).

From Fig. 4 we notice that either in the absence or in the presence of wetting, the finger competition function $C(n,t)$

assumes only negative values for $t > 0$. From our discussion above this would indicate favored finger competition among the inward pointing fingers of the less viscous, penetrating fluid. Moreover, it is also evident that this finger competition should be less intense (but not absent) when wetting effects are of importance (dashed curve is far below the solid one for longer times). In other words, we can say that by neglecting wetting effects one would be overestimating finger competition among inward moving fingers. As expected, the predictions of Fig. 4 are in full agreement with the finger competition behavior observed in Figs. 2 and 3, reinforcing the validity of our finger competition mechanism.

3.2 The shape of the fingers

Here we study a mechanism that controls the finger shape behavior at the weakly nonlinear level. Once again we describe this particular nonlinear feature by considering the coupling of a small number of modes[20]. It turns out that finger tip-narrowing and tip-broadening phenomena can be described by considering the influence of a fundamental mode n on the growth of its harmonic $2n$. Under these circumstances, the equations of motion for the cosine and sine modes of the harmonic are

$$\dot{a}_{2n} = \lambda(2n)\, a_{2n} + \frac{1}{2}\, T(n,t)\, a_n^2, \tag{17}$$

$$\dot{b}_{2n} = \lambda(2n)\, b_{2n}, \tag{18}$$

where

$$T(n,t) = \left\{ F(2n,n) + \lambda(n)\, G(2n,n) + H(2n)\lambda(n)\left[\lambda(n) + \frac{\dot{b}}{2b}\right]\right\}, \tag{19}$$

is the finger tip function. From Eq. (18) we can see that the growth of the sine mode b_{2n} is uninfluenced by a_n, and does not present second-order couplings, so we focus on the growth of the cosine mode. The interesting point about the function $T(n,t)$ is that it controls the finger shape behavior. The sign of $T(n,t)$ dictates whether finger tip-widening or finger tip-narrowing is favored by the dynamics. From Eq. (17) we see that if $T(n,t) > 0$, the result is a driving term of order a_n^2 forcing growth of $a_{2n} > 0$, the sign that is required to cause inward-pointing fingers to become wide, favoring finger tip-broadening. In contrast, if $T(n,t) < 0$ growth of $a_{2n} < 0$ would be favored, leading to inward-pointing finger tip-narrowing.

To analyze the influence of wetting on the shapes of both inward and outward pointing fingers at second-order, in Fig. 5 (on the top) we plot the behavior of $T(n,t)$ as a function of time, for the coupling between two Fourier modes ($n = 20$ and $2n = 40$). This is done for the situations in which wetting is neglected ($\gamma = 0$, dashed curve) and taken into account ($\gamma = 2/3$, solid curve). Once again, the parameters used to plot this figure are exactly the ones utilized in Figs. 2 and 3. We readily verify that the finger tip function $T(n,t)$ is always positive regardless the value of γ. From our previous discussion about the role of $T(n,t)$ this would indicate that the inward pointing fingers should be wider than the outward pointing fingers. However, we see that the $T(n,t)$ curve in the presence of wetting (solid curve) lies considerably above the corresponding curve (dashed curve) when wetting is absent. This means that in the presence of wetting the inward pointing fingers would be significantly wider than those formed in the absence of wetting.

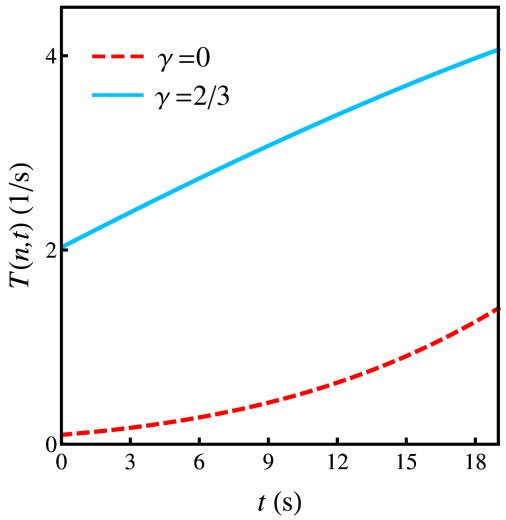

Fig. 5 Variation of the finger tip function $T(n,t)$ with time t. The dashed (solid) curves are plotted for $\gamma = 0$ ($\gamma = 2/3$).

As a matter of fact, this is exactly the behavior previously shown in the closed-up sections of the interfaces depicted in Figs. 2(b) and 3(b). By examining these figures it is evident that when $\gamma = 2/3$ the inward pointing fingers are much wider than the outward pointing fingers. In addition, the resulting fingering structures arising when $\gamma = 2/3$ are shorter than the ones produced when $\gamma = 0$. All these findings support the idea that wetting effects have an important effect on the shape of both inward and outward pointing fingers.

4 Conclusions

Existing theoretical and experimental studies have shown that wetting effects can be of importance to the understanding of the pattern formation dynamics in injection-driven[10–17,23] and centrifugally-induced[30] flows in Hele-Shaw cells. In this work, we add to this list of investigations, by examining the

role of wettability in determining the morphology of emerging pattern-forming structures under lifting Hele-Shaw flow circumstances. In this scenario, we consider the flow of a viscous wetting fluid surrounded by a less viscous nonwetting one in a Hele-Shaw cell for which the upper plate can be lifted, so that its gap-width is time-dependent.

We tackled the problem by performing a perturbative weakly nonlinear analysis of the system up to second-order. This method permits exploration of relevant nonlinear features of the sucked fluid-fluid interface analytically. Our theoretical results indicate that wetting effects can be of great impact on the resulting pattern morphologies. More specifically, we predicted the formation of patterns in which fingers compete, leading to the formation of interfacial shapes where short, blunt fingers of the nonwetting outer fluid are alternated by short sharp fingers of the wetting inner fluid. We have shown that the basic pattern forming mechanisms connected to such peculiar nonlinear aspects of the interface can be revealed and qualitatively interpreted through the coupling of a few participating interfacial Fourier modes. These theoretical predictions do capture the most salient morphological features detected in lifting Hele-Shaw flow experiments[32–38]. If wetting effects are neglected, the final patterned structures would present an overestimated competition, while the inward pointing fingers would be just slightly wider than the outward pointing ones.

Confirmation of our predictions and access to additional information about the suggestive nonlinear aspects identified in this analytic work should be possible from new laboratory experiments as well as fully nonlinear numerical simulations of the lifting problem that focus on circumstances in which wetting effects are of relevance.

We thank CNPq for financial support through the program "Instituto Nacional de Ciência e Tecnologia de Fluidos Complexos (INCT-FCx)", and FACEPE through PRONEM project No. APQ-1415-1.05/10.

References

1 P. G. de Gennes, *Rev. Mod. Phys.*, 1985, **57**, 827–863.
2 F. Melo, J. F. Joanny and S. Fauve, *Phys. Rev. Lett.*, 1989, **63**, 1958–1961.
3 J. A. Diez and L. Kondic, *Phys. Rev. Lett.*, 2001, **86**, 632–635.
4 M. A. Fardin, O. M. Rossier, P. Rangamani, P. D. Avigan, N. C. Gauthier, W. Vonnegut, A. Mathur, J. Hone, R. Iyengar and M. P. Sheetz, *Soft Matter*, 2010, **6**, 4788–4799.
5 P. G. Saffman and G. Taylor, *Proc. R. Soc. Lond. A*, 1958, **245**, 312–329.
6 G. M. Homsy, *Annual Review of Fluid Mechanics*, 1987, **19**, 271–311.
7 K. McCloud and J. Maher, *Physics Reports*, 1995, **260**, 139 – 185.
8 J. Casademunt, *Chaos: An Interdisciplinary Journal of Nonlinear Science*, 2004, **14**, 809–824.
9 C.-W. Park and G. M. Homsy, *J. Fluid Mech.*, 1984, **139**, 291–308.
10 P. Tabeling and A. Libchaber, *Phys. Rev. A*, 1986, **33**, 794–796.
11 L. Schwartz, *Physics of Fluids (1958-1988)*, 1986, **29**, 3086–3088.
12 P. G. Saffman, *J. Fluid Mech.*, 1986, **173**, 73–94.
13 D. A. Reinelt, *Physics of Fluids (1958-1988)*, 1987, **30**, 2617–2623.
14 D. A. Reinelt, *J. Fluid Mech.*, 1987, **183**, 219–234.
15 T. Maxworthy, *Phys. Rev. A*, 1989, **39**, 5863–5866.
16 L. M. Martyushev and A. I. Birzina, *Journal of Physics: Condensed Matter*, 2008, **20**, 045201.
17 E. O. Dias and J. A. Miranda, *Phys. Rev. E*, 2013, **88**, 013016.
18 L. Paterson, *J. Fluid Mech.*, 1981, **113**, 513–529.
19 J.-D. Chen, *J. Fluid Mech.*, 1989, **201**, 223–242.
20 J. A. Miranda and M. Widom, *Physica D: Nonlinear Phenomena*, 1998, **120**, 315 – 328.
21 J. Mathiesen, I. Procaccia, H. L. Swinney and M. Thrasher, *EPL (Europhysics Letters)*, 2006, **76**, 257.
22 S. Li, J. S. Lowengrub, J. Fontana and P. Palffy-Muhoray, *Phys. Rev. Lett.*, 2009, **102**, 174501.
23 P. H. A. Anjos and J. A. Miranda, *Phys. Rev. E*, 2013, **88**, 053003.
24 L. W. Schwartz, *Physics of Fluids A: Fluid Dynamics (1989-1993)*, 1989, **1**, 167–169.
25 L. Carrillo, F. X. Magdaleno, J. Casademunt and J. Ortín, *Phys. Rev. E*, 1996, **54**, 6260–6267.
26 E. Alvarez-Lacalle, J. Ortín and J. Casademunt, *Physics of Fluids (1994-present)*, 2004, **16**, 908–924.
27 J. A. Miranda and E. Alvarez-Lacalle, *Phys. Rev. E*, 2005, **72**, 026306.
28 R. Folch, E. Alvarez-Lacalle, J. Ortín and J. Casademunt, *Phys. Rev. E*, 2009, **80**, 056305.
29 C.-Y. Chen, Y.-S. Huang and J. A. Miranda, *Phys. Rev. E*, 2011, **84**, 046302.
30 E. Álvarez-Lacalle, J. Ortín and J. Casademunt, *Phys. Rev. E*, 2006, **74**, 025302.
31 M. J. Shelley, F.-R. Tian and K. Wlodarski, *Nonlinearity*, 1997, **10**, 1471.
32 S. Roy and S. Tarafdar, *Phys. Rev. E*, 1996, **54**, 6495–6499.
33 M. Tirumkudulu, W. B. Russel and T. J. Huang, *Physics of Fluids (1994-present)*, 2003, **15**, 1588–1605.
34 D. Derks, A. Lindner, C. Creton and D. Bonn, *Journal of Applied Physics*, 2003, **93**, 1557–1566.
35 S. Poivet, F. Nallet, C. Gay, J. Teisseire and P. Fabre, *The European Physical Journal E*, 2004, **15**, 97–116.
36 M. B. Amar and D. Bonn, *Physica D: Nonlinear Phenomena*, 2005, **209**, 1 – 16.
37 A. Lindner, D. Derks and M. J. Shelley, *Physics of Fluids (1994-present)*, 2005, **17**, 072107.
38 J. Nase, D. Derks and A. Lindner, *Physics of Fluids (1994-present)*, 2011, **23**, 123101.
39 E. O. Dias and J. A. Miranda, *Phys. Rev. E*, 2013, **88**, 043002.
40 S. Sinha, T. Dutta and S. Tarafdar, *The European Physical Journal E*, 2008, **25**, 267–275.
41 J. A. Miranda and M. Widom, *International Journal of Modern Physics B*, 1998, **12**, 931–949.
42 F. P. Bretherton, *J. Fluid Mech.*, 1961, **10**, 166–188.